

Parameters of Neutron Resonances in $^{232}\text{Th}\dagger$

M. R. BHAT AND R. E. CHRIEN

Brookhaven National Laboratory, Upton, New York

(Received 5 October 1966)

The neutron widths and radiation widths of the four lowest S -wave resonances in thorium, $E_0=21.7$, 23.4, 59.4, and 69.1 eV, have been measured using transmission techniques. A mean value of Γ_γ of 20.1 ± 1.3 meV is obtained for these four measurements. Using these parameters, the resonance capture integral for thorium is computed and found to be 86 ± 6 b, in substantial agreement with recent measurements. No evidence is found for a fluctuating component of Γ_γ within the experimental error. The methods of analysis, including the use of a non-Gaussian resolution function, are described.

I. INTRODUCTION

BECAUSE of the importance of thorium in breeder-reactor technology, there is considerable interest in its nuclear parameters. Recently, measurements on the neutron resonance parameters¹⁻⁵ and on the resonance capture integral have been reported.^{6,7} Much of the recent effort has been concentrated on a precise determination of the radiation widths for resonances in thorium and on increased precision in the determination of the neutron widths of the low-energy resonances. Since well over half of the resonance capture integral is accounted for by the three lowest-lying S -wave resonances, the agreement between the calculated and measured values of the resonance integral is critically affected by the parameters of these resonances.

The present work was undertaken to provide an independent set of parameters for the first four S -wave resonances in thorium and to verify the surprisingly low—compared to earlier measurements—radiation widths reported recently.

In this work transmission methods have been used exclusively. The recently reported Harwell³ studies employ scattering and capture techniques in addition to transmission measurements, while the General Atomic⁴ work employs capture techniques alone. The advantage of the transmission technique lies mainly in the absence of troublesome systematic errors associated with partial cross-section measurements. These errors include the effects of multiple scattering in the sample, the necessity of calibrating the incoming beam intensity, and the problems of measuring the energy variation of the efficiency of a γ -ray detector. Furthermore, in

principle, a transmission measurement on an even- A target, ($I=0$), such as ^{232}Th , is adequate to determine all resonance parameters, since the statistical weight g is unity.

The Doppler effect on the rather narrow resonances of thorium precludes the use of shape analysis, and so the area above the resonance dip must be measured as a function of sample thickness to deduce the neutron width and total width for the resonance. While free of the various systematic errors associated with partial cross section measurements, the transmission-area method requires accurate and consistent determinations for several thicknesses, and the sensitivity of the method for radiation width determination is poor when $\Gamma_n \gg \Gamma_\gamma$. Fortunately, in the range of application discussed here the latter restriction is not a factor.

With the beam intensity and resolution available at the BGRR fast chopper, precise cross-section measurements are restricted to energies below about 100 eV, hence no analysis of the higher-energy resonances in thorium was attempted.

II. EXPERIMENTAL EQUIPMENT AND TECHNIQUES

The transmissions were measured with the BNL fast chopper located at the Brookhaven Graphite Research Reactor. A flight path of 29.74 m through three sections of He-filled balloons in combination with a chopper burst width of 1.0 μsec yielded a nominal resolution of 50 nsec/m (see, however, later discussion of resolution function). A boral-shielded bank of 384 counter tubes in a common BF_3 atmosphere detected neutrons with an efficiency of the order of 10% in the energy range of this experiment. The boral shield reduced the efficiency of the detector to neutrons of below 5-eV energy to essentially zero to maintain a low room background.

Samples of thorium foil approximately 2.0 in. \times 2.0 in. were mounted in a sample cyler located at the exit stator of the chopper. Dummy (open) and background positions were also located on this cyler, which cycled through these positions with a 20-min period. Ratios of sample "in time" to sample "out time" were adjusted for optimum statistical accuracy. The background was taken by a 3-in. Lucite plug on the cyler.

The cyler was electronically linked to an SDS-910

\dagger This work was supported by the U. S. Atomic Energy Commission.

¹ *Neutron Cross Sections*, compiled by D. J. Hughes and R. B. Schwartz (U. S. Government Printing Office, Washington, D. C.), 2nd ed., Vol. III, Z-88 to 98, BNL 325, Suppl. No. 2 (1965).

² J. B. Garg, J. Rainwater, J. S. Petersen, and W. W. Havens, Jr., *Phys. Rev.* **134** B985 (1964).

³ M. Asghar, C. M. Chaffey, M. C. Moxon, N. J. Pattenden, E. R. Rae, and C. A. Uttley, *Nucl. Phys.* **76**, 196 (1966).

⁴ E. Haddad, S. J. Friesenhahn, F. H. Frohner, and W. M. Lopez, *Phys. Rev.* **140**, B50 (1965).

⁵ P. Ribon, M. Sanche, H. Derrien, and A. Michaudon, in *Proceedings of the International Conference on Study of Nuclear Structure with Neutrons, Antwerp* (North-Holland Publishing Company, Amsterdam, 1966), p. 565.

⁶ W. K. Foell and T. J. Connolly, *Nucl. Sci. Eng.* **21**, 406 (1965).

⁷ M. Brose, *Nucl. Sci. Eng.* **19**, 244 (1964).

TABLE I. Sample thicknesses.

Nominal thickness (inches)	Sample thickness (atoms/barn)	No. of independent runs
0.002	0.1545×10^{-3}	2
0.010	0.7623×10^{-3}	2
0.040	0.2960×10^{-2}	3
0.125	0.9236×10^{-2}	3
0.375	0.2791×10^{-1}	2

computer data gathering system, which has been described in detail.⁸ Sample-in and sample-out spectra were recorded in 512 channel segments in the computer memory. Additionally recorded were monitor counts, background, elapsed times, and chopper speed. The computer, which was time-shared among three experiments, was also used for data reduction, as will be described in some detail in a later section. The recording time for a time-of-flight event was approximately 100 μsec . No deadtime corrections were necessary at the event rates recorded in this work (20 to 30 counts/sec).

Samples of thorium were obtained in the form of foils approximately 2×2 in. and of nominal thickness of 0.002, 0.010, 0.040, 0.125, and 0.375 in. Each foil was radiographed for detection of voids or nonuniformities, and the foils were spectrographically checked for impurities. Several runs were made on each foil to check the consistency of the measurements. A total of 12 runs were made on all samples. Table I lists the thickness of each sample foil as determined by weight and area measurements and the number of independent runs made with each.

III. ANALYTICAL METHODS

General Description

Although the experimental procedures in a transmission measurement are straightforward, the goal of measuring the parameters of thorium to the highest possible accuracy makes a careful and occasionally tedious analysis of the data a necessity. In this section a summary is given of the analysis of the thorium transmissions.

After accumulation of the time-of-flight data from a typical experiment, three storage media could be used for the data: (1) magnetic tape, (2) paper tape, and (3) typewritten sheet. A magnetic-tape library was retained for all runs of this series. Paper tape proved useful because of the availability of tape-to-card conversion equipment. Occasionally the typewritten sheet was useful for various hand calculations.

Figure 1 has been drawn to show schematically the flow of data through the processing steps of this experiment. After accumulation the time-of-flight spectra were recorded and stored on magnetic tape. Soon there-

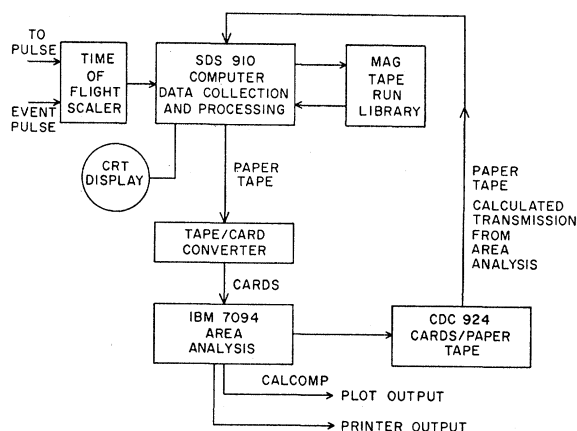


Fig. 1. The various stages of the processing of the data of this experiment. The SDS 910 is used for data collection, intermediate processing, and comparison with theoretical predictions. The 7094 is used for area analysis. Cards from the results of area analysis can be converted to paper tape at the CDC 924 and fed back into the SDS 910 for comparison with experiment.

after they were recalled from tape and processed to produce transmission data in the SDS-910. This step involves smoothing, least-squares curve fitting for the open spectrum, background subtraction, and channel-by-channel division of the sample spectrum by the open spectrum. Every stage in this process could be observed visually on the cathode-ray tube (CRT) display. Figure 2(a) shows a photograph of the CRT display of the open and sample spectra of a $\frac{1}{8}$ -in. Th foil shown side by side. In Fig. 2(b) the spectra are shown after fitting a second-degree polynomial to the open spectrum and normalizing. Figure 2(c) shows the final computed transmission from 75 to 20 eV. Any of these manipulations of the data could be carried out without interruption of the data-collection functions of the computer.

The analysis of transmission dips is not conveniently carried out in the SDS-910 because of its limited memory size and speed. The transmissions were punched out on tape, converted to cards, and submitted to the centrally located IBM-7094 at Brookhaven. A modified Atta-Harvey^{9,10} area-analysis code was employed to analyze the dip areas and to produce a computed transmission curve from the deduced resonance parameters. If desired, a Calcomp plot, such as Fig. 6, showing the observed and calculated transmissions, could be produced by the 7094. For an analysis involving the effect of resolution function of the system, it was desirable to feed the calculated transmissions back to the SDS-910 for direct comparison to the data. This was done using a CDC-924 for conversion to paper tape which could be read by the SDS-910.

⁹ R. E. Chrien, Phys. Rev. **141**, 1129 (1966).

⁸ R. Chrien, S. Rankowitz, and R. Spinrad, Rev. Sci. Instr. **35**, 1150 (1964).

¹⁰ S. Atta and J. A. Harvey, U. S. Atomic Energy Commission Report No. ORNL 3205, Oak Ridge National Laboratory, 1961 (unpublished).

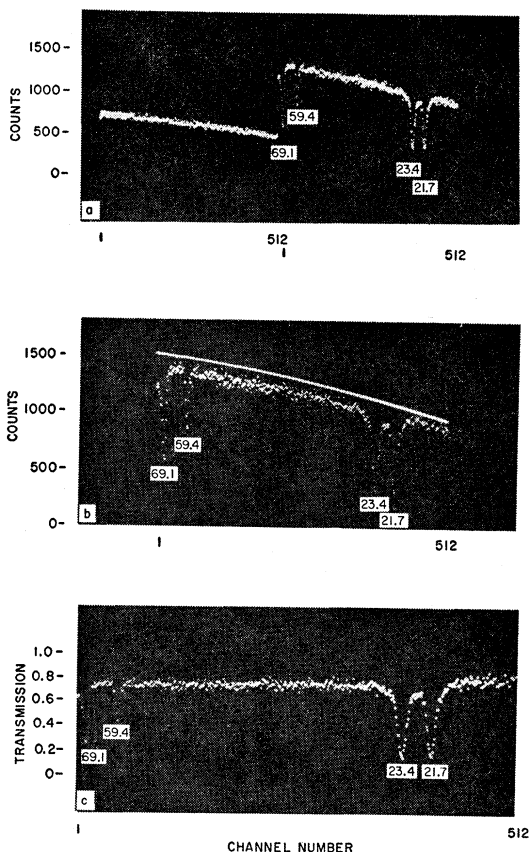


FIG. 2(a). The sample-out and sample-in time-of-flight spectra for the $\frac{1}{8}$ -in.-thick thorium sample. The open spectrum run time was approximately half of the sample run time. Each spectrum contains 512 0.5- μ sec channels, and the resonance energies are shown in eV. (b) The sample-out and sample-in spectra are shown after fitting a second degree polynomial to the open spectrum and normalizing to the equivalent running time of the sample spectrum. The spectra are shown superposed. (c) The computed transmission obtained from spectra of Fig. 2(b). The energy range shown is from about 75 to 20 eV.

Open-Spectrum Treatment

Before obtaining the sample transmission, a second-degree polynomial of the form

$$N(t) = K_0 + K_1 t + K_2 t^2$$

was fitted to the open spectrum. It has been established over a lengthy period of examination that such a polynomial is an adequate representation of the incident spectrum over the energy region of this experiment.

Background and Normalization

Separate experiments have shown that the background is independent of time-of-flight except near $t=0$. This flat background is computed from the totalized background events over all channels recorded over the duration of the run. A typical background rate is 10% of the open beam spectrum.

All normalizations were performed using elapsed time ratios. Drifts in electronic sensitivities or beam intensities were eliminated by the rapid cycling of the samples.

Resolution-Function Corrections

It is often asserted that no knowledge of the resolution function of the system is needed in an area analysis. There are, however, second-order corrections which arise from the asymmetry of the resolution function and the resonance, and the necessity to measure only the fraction of the dip area lying between certain "wing cuts" with a correction for the area lying outside these cuts. These errors tend to be larger for thick samples since a larger fraction of the area tends to lie outside the wing cuts. They tend also to be large when resonances lying close together make it necessary to employ narrow wing cuts.

In the usual area analysis (as exemplified by the Atta-Harvey code), a Gaussian resolution function is assumed, whose width is a combination of time-dependent and time-independent parts, namely,

$$R^2 = R_0^2 + R_1^2 t^2, \quad (1)$$

where R_0 is a constant determined by the burst width channel width and detector jitter; and $R_1 t$ is proportional to the time-of-flight t and is introduced by the

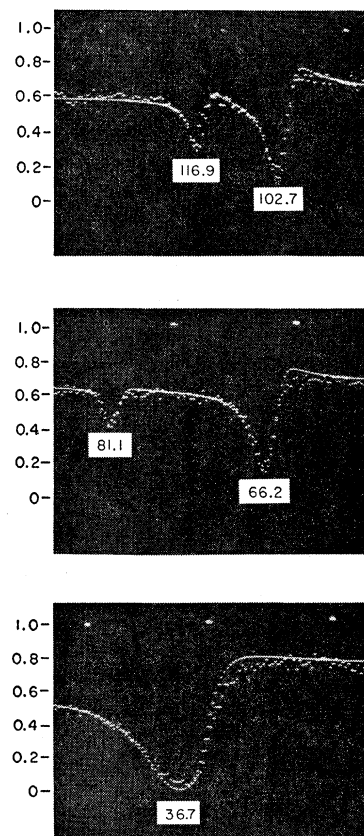


FIG. 3. Time-of-flight spectra for five resonances in ^{238}U at $E_0 = 117, 103, 81, 66,$ and 37 eV. The fitted curves show clearly discrepancies between measured and calculated transmissions, particularly at or near the maximum and minimum transmission regions.

finite size of the detector and consequent uncertainty in flight time.

However, a careful examination of the transmission data obtained with our experimental arrangement indicated that the use of the Gaussian function with the Atta-Harvey code did not adequately reproduce our data. The possibility of a "tail" in the resolution function arises quite naturally in any time-of-flight experiment from neutrons which reach the detector after one or more scatterings in material near the flight path or the detector. The recorded events in any time channel contain, therefore, a contribution from neutrons of higher energies than that appropriate to that channel. If we make the simplifying assumption that a uniform probability density function adequately describes these degraded neutrons down to a lower time-of-flight cutoff, we can write

$$N_{\text{corr}}(t) = \sum_{n=0}^{\nu} \frac{1}{1-\beta} \left[\delta_{0n} - \frac{\beta}{\nu} (1-\delta_{0n}) \right] N(t-nT), \quad (2)$$

where $N_{\text{corr}}(t)$, corrected number of events at time channel t , $N(t)$, observed number at time t , T , channel width, β , fraction of beam represented by degraded neutrons, ν , spread in arrival time, in channels, for degraded neutrons, and δ , Kronecker delta. The quantities β and ν were determined from a separate transmission experiment on a $\frac{1}{4}$ -in.-thick piece of ^{238}U .

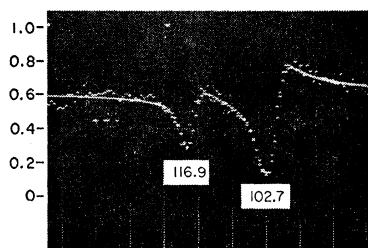


FIG. 4. Spectra similar to those of Fig. 3, except for the use of a non-Gaussian resolution function, which clearly improves the fit.

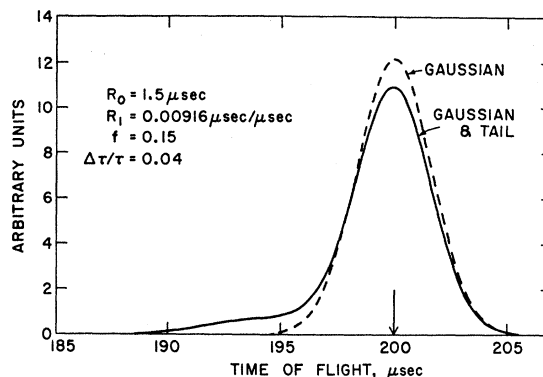
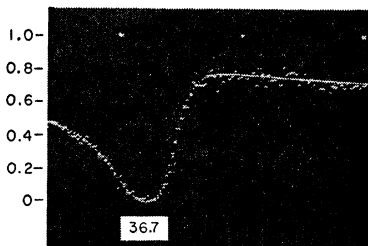
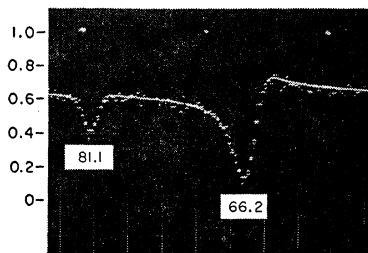


FIG. 5. The deduced resolution function for this experiment evaluated at $t=200$ μsec , evaluated under the assumptions of Eq. (2).

The experimental points were compared directly to transmissions calculated from the known parameters¹ of ^{238}U using the Atta-Harvey code and feeding the results into the SDS-910. By inspecting the comparison visually on the CRT display values of β and ν were determined rapidly by trial and error, through a program which allowed the above correction to be applied to the experimental points.

Figure 3 shows the discrepancies between the experimental and predicted transmission curves of five resonances in ^{238}U . Figure 4 shows the comparison after correction for the non-Gaussian part of the resolution function. Figure 5 shows the deduced resolution function for the chopper system at $E=115$ eV for the values determined in the ^{238}U experiment, $\beta=0.15\pm 0.03$ and $\nu=16\pm 4$. The data of the thorium experiment have therefore been corrected for the non-Gaussian tail by application of Eq. (2).

A discussion of asymmetric resolution functions similar to the one above may be found in Ref. 11.

Area Analysis

After the resolution function corrections described above the Atta-Harvey area analysis code was used to extract a set of resonance parameters from a resonance dip. The BNL version of this code has been previously described.⁹ For the present analysis a further modification was introduced to provide a more rapid convergence of the results and to lessen the dependence of the parameters on the (arbitrary) position of the wing cuts. In the usual version (see Ref. 10) the resonance parameters are varied according to the restriction:

$$\text{Const} = \sum_{i=m}^n T_i(\text{exp}) = \sum_{i=m}^n T_i(\text{calculated}). \quad (3)$$

We have modified this condition so that

$$\text{Const} = \sum w_i T_i(\text{exp}) = \sum w_i T_i(\text{calculated}), \quad (4)$$

¹¹ M. Bhat, R. Chrien, and I. Cole, Proceedings of the Conference on Neutron Cross Section Technology, Washington, D. C., USAEC CONF-660303, 1966 (unpublished).

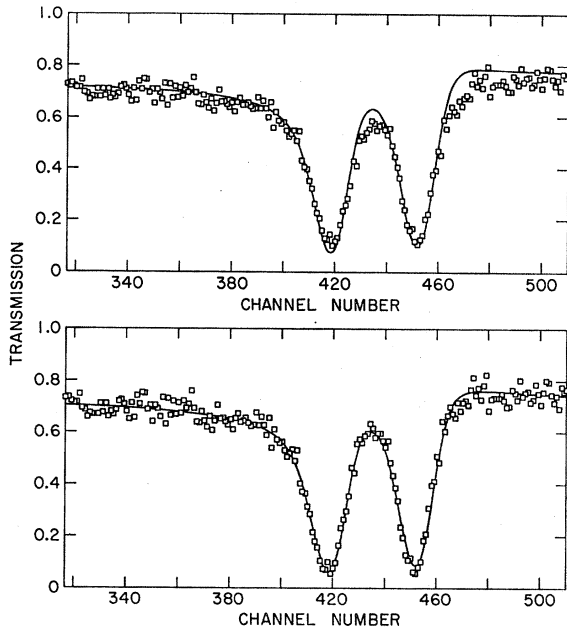


FIG. 6. The $\frac{3}{8}$ -in.-thick thorium transmission fitted in the region near the 21- and 23-eV resonances. The uncorrected transmissions are shown above and the transmissions corrected for the non-Gaussian component in the resolution function are shown below.

where the weights w_i are distributed on a Gaussian curve of FWHM (full width at half-maximum) equal to the FWHM of the observed transmission dip.

$$w_i = \frac{e^{-(n_i - n_0)^2 / 2\sigma^2}}{\sum_i e^{-(n_i - n_0)^2 / 2\sigma^2}}, \quad (5)$$

where n_i are the time channels and n_0 is the time channel at the resonance energy.

The effect of such a weighting is to increase the importance of the points near the peak cross section and to decrease the effect of statistical fluctuations in the points near the wings of the resonance.

For each run analyzed in the above manner, the sample transmission as calculated from the derived resonance parameters in the region 80 to 20 eV was compared to the experimental data. A satisfactory fit to the data was demanded over this entire energy range. An example of such a fit is shown in Fig. 6, a plot of measured and calculated transmissions for one of the $\frac{3}{8}$ -in. sample runs.

A value of the potential scattering cross section, σ_{pot} , of 11.4 barns⁴ was assumed for all runs. This value is in satisfactory agreement with our thick-sample data.

The Area Function

Several methods have been developed for combining transmission dip areas for various sample thicknesses to produce a single set of consistent resonance param-

TABLE II. Summary of results.

E_0^a (eV)	Γ_n (meV)	Γ (meV)	Γ_γ (meV)	$\text{cov}(\Gamma_n, \Gamma) / \delta\Gamma_n \delta\Gamma$
21.78	2.61 ± 0.17	24.97 ± 2.1	22.4 ± 2.4	-0.73
23.45	4.17 ± 0.25	26.21 ± 2.2	22.0 ± 2.6	-0.82
59.46	4.41 ± 0.27	20.6 ± 2.9	16.2 ± 2.3	-0.74
69.13	42.86 ± 2.6	64.3 ± 3.7	21.5 ± 4.7	-0.88

^a The quoted resonance energies of this table are from Ref. 1, BNL 325 recommended values.

eters. These are all variations of the thin-thick method.¹² The method used in the present work has been previously summarized.¹⁰ A nonlinear least-squares fitting technique is used to calculate the set of parameters producing the best fit to the sum of transmissions between wing cuts

$$S(n, \Gamma_n, \Gamma) = \int_{E_1}^{E_2} e^{-n\sigma\Delta(\Gamma_n, \Gamma)} dE \quad (6)$$

over the range of sample thicknesses considered. The computed, rather than measured, transmission values as derived from the Atta-Harvey code are used in this analysis. This procedure eliminates the perturbing effects of neighboring resonances on the area measurements. The best values of Γ_n and Γ are derived with their errors and covariance. From these quantities the radiation width and its associated error may be derived.

$$\Gamma_\gamma = \Gamma - \Gamma_n, \quad \delta\Gamma_\gamma^2 = \delta\Gamma^2 + \delta\Gamma_n^2 - 2 \text{cov}(\Gamma, \Gamma_n), \quad (7)$$

where $\text{cov}(\Gamma, \Gamma_n)$ is the covariance.

The values of Γ_n and Γ corresponding to a minimum of the χ^2 function formed from the $S(n, \Gamma_n, \Gamma)$ functions were determined along with their errors and covariance. The error terms quoted are

$$\delta^2\Gamma_n = E_{11}(\chi^2)_{\text{min}}/F \quad \text{and} \quad \delta^2\Gamma = E_{22}(\chi^2)_{\text{min}}/F,$$

where E_{11} and E_{22} are the diagonal terms of the error matrix and F denotes the number of degrees of freedom.

Figure 7 shows the results of this fit for the 69-eV resonance. There are 11 different runs on 5 different sample thicknesses included. Each of the four resonances analyzed in the present work was treated in similar manner.

IV. RESULTS

The results of this experiment are summarized in the parameters of Table II.

The mean value of Γ_γ derived from these four resonances is 20.1 ± 1.3 meV and is in substantial agreement with the mean values reported by Harwell³ of 21.5, that of General Atomic⁴ of 24.5, and Columbia², 19 meV. This is to be compared with the older value of 34 meV reported in BNL 325. The large value of 30 meV

¹² D. J. Hughes, J. Nucl. Energy 1, 237 (1955).

reported by Harwell for the radiation width of the 23-eV resonance is not confirmed here. There is no evidence in the present work for a fluctuating component of the radiation width as has been suggested by the Harwell work.

The neutron widths reported in Table II are derived principally from the thin-sample area measurements, since the area function for a thin sample is relatively independent of the assumed total width. In the least-squares fitting procedure of the previous section a relative weight of 10 to 1 was assigned to the thin sample point over the other sample thicknesses in order to force a fit through this point. This procedure was desired to avoid introduction of possible systematic errors from the thicker sample points into the neutron width determination. The neutron widths for the first two levels are somewhat higher than those reported by General Atomic and Harwell, and more in accord with the older values of BNL 325, 2nd edition.

We may compare the recent measurements of the thorium parameters by their effects on the calculation of the dilute-resonance integral. The most recent measurements of the latter quantity are reported in BNL 325, 2nd ed., Suppl. No. 2, Vol. II where a mean value of 83 ± 3 b, including a $1/v$ contribution of 3 b is listed.

The resonance-capture integral (in barns) may be computed from the relation

$$I = \sum_r \frac{4090 \Gamma_n \Gamma_\gamma}{E_0^2 \Gamma} + \delta_{l=0} + \delta_{l=1},$$

where the widths are given in meV, E_0 is given in eV, \sum represents a sum over resolved resonances, and $\delta_{l=0}$ and $\delta_{l=1}$ represent contributions from higher-energy S- and P-wave resonances. It can be easily shown that $\delta_{l=0}$ and $\delta_{l=1}$ have the following forms:

$$\delta_{l=0} = 2C_0 S_0 \bar{F}_0 \int_{\sqrt{E}}^{\infty} \frac{dx}{x^2(rx+1)}, \quad (8)$$

$$\delta_{l=1} = 2C_1 S_1 \bar{F}_1 \int_0^{\infty} \frac{dx}{1+\alpha x^2+r\alpha x^3}. \quad (9)$$

$\delta_{l=0}$ may be readily evaluated by elementary integration, while $\delta_{l=1}$ is somewhat more difficult, but as Dresner¹⁴ points out may be approximated by ignoring the αx^2 term in the denominator.

The following symbols in the above are defined as

¹³ M. Bhat and R. E. Chrien, in *Proceedings of the International Conference on Study of Nuclear Structure with Neutrons, Antwerp, 1965* (North-Holland Publishing Company, Amsterdam, 1966), p. 523.

¹⁴ L. Dresner, *Resonance Absorption in Nuclear Reactors* (Pergamon Press, Ltd., Oxford, England, 1960), p. 97.

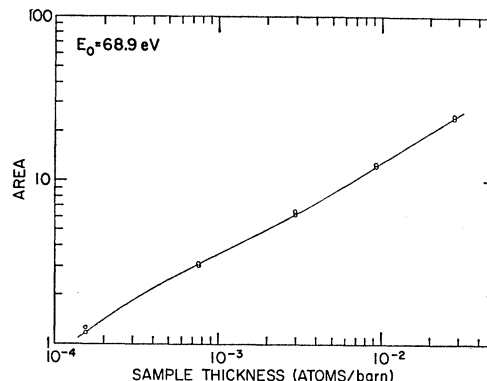


FIG. 7. The least-squares area function is shown for the 69-eV thorium resonance. Eleven runs involving five different sample thicknesses are shown. The y co-ordinate is proportional to the transmission dip area,

$$A = \int_{E_1}^{E_2} (1-T)dE.$$

follows:

$$C_0 = 411.0 \text{ b eV}^{1/2},$$

$$S_0 = S\text{-wave strength function} \approx 0.7 \times 10^{-4},$$

$$\bar{F}_0 = \text{fluctuation factor} \left\langle \left\langle \frac{\Gamma_n}{\Gamma_n + \Gamma_\gamma} \right\rangle \right\rangle / \frac{\langle \Gamma_n \rangle}{\langle \Gamma_n \rangle + \langle \Gamma_\gamma \rangle},$$

$$r = \langle \Gamma_n^0 \rangle / \Gamma_\gamma,$$

$$\alpha = 3.167 \times 10^{-6},$$

$$C_1 = 3.9 \times 10^{-3} \text{ b eV}^{-1/2};$$

thus,

$$\delta_0 = 2C_0 S_0 \bar{F}_0 \left[\frac{1}{\sqrt{E_1}} - r \ln \frac{1+r\sqrt{E_1}}{r\sqrt{E_1}} \right], \quad (10)$$

$$\delta_1 \approx \frac{4\pi}{3\sqrt{3}} C_1 \bar{F}_1 S_1 / (r\alpha)^{1/3}. \quad (11)$$

The evaluation of these correction terms requires the knowledge of certain average parameters. We have adopted

$$\langle \Gamma_\gamma \rangle = 20 \text{ meV, present experiment,}$$

$$S_0 = 0.69 \times 10^{-4}, \text{ Columbia}^2,$$

$$D = 17.5 \text{ eV, Columbia.}$$

The P-wave strength function is not well known; values from 0.5 to 2.6×10^{-4} have been reported.^{3,15} We have adopted the value 1.0×10^{-4} . The fluctuation factor varies with the ratio Γ_n/Γ_γ . We have adopted the values 0.7 and 0.8 for δ_0 and δ_1 , respectively.

Three sets of experimental results are considered here, and a fourth set is used to help evaluate δ_0 . More than

¹⁵ L. M. Bollinger and G. E. Thomas, *Phys. Letters* 8, 45 (1964).

TABLE III. Table of resonance integral calculations, in barns.

	Present work	General Atomic	Harwell
I Resolved resonance region	62.78 (0.5-70 eV)	71.88 (0.5-222)	71.22 (0.5-866 eV)
II Columbia data to 4000 eV	18.34 (70-4000 eV)	8.16 (222-4000 eV)	1.70 (866-4000 eV)
III Unresolved S-wave contribution above 4000 eV	1.0	1.0	1.0
IV P-wave contribution	1.2	1.2	1.2
V 1/v contribution	3.0	3.0	3.0
Totals	86±6	85.2	78.2

half of the resonance integral is contributed by the first three resonances in thorium and 80% by the resonances below 200 eV.

(1) The presently reported results are combined with the Columbia results from 100 to 4000 eV to calculate the resonance integral. A $\langle\Gamma_\gamma\rangle$ of 20 meV is assumed.

(2) The Harwell results are combined with Columbia results above 866 eV.

(3) The General Atomic data are combined with Columbia data above 222 eV.

In each instance the Columbia data is used to 4000 eV. Above that energy the integrated expressions (10) and (11) are used to provide corrections.

The results are listed in Table III. The resonance integral has been computed using the quoted parameters for Γ_n and Γ_γ . Where Γ_γ has not been measured, an average value of Γ_γ as measured in the *same experiment* has been used (e.g., $\langle\Gamma_\gamma\rangle=19$ meV for the Columbia high-energy data). Of course, any value of the resonance integral may be obtained by an arbitrary choice of an average Γ_γ . This, however, leads, in general, to an inconsistent set of Γ_n and Γ_γ for a measured resonance and so we must reject this procedure.

The higher values obtained for the BNL data arise from the higher values for the neutron widths of the first two resonances.

ACKNOWLEDGMENTS

The authors gratefully acknowledge the assistance of I. W. Cole and J. Domish in performing the computations and data analysis.

Neutron-Capture Gamma-Ray Studies in Isotopes of Tungsten

ROBERT R. SPENCER AND KENNETH T. FALER

*Idaho Nuclear Corporation, Idaho Falls, Idaho**

(Received 6 September 1966)

γ -ray spectra from a natural-tungsten target following the capture of 0.06-eV neutrons and neutrons corresponding in energy to the lowest-energy resonances in W^{182} , W^{183} , and W^{186} have been obtained at high resolution using a lithium-drifted germanium detector. Transitions have been identified which take place from the capture states to states near ground states in the final nuclei. Low-lying states previously known have been observed and several new states have been identified. Precise energy values and approximate relative intensities of the transitions are given.

I. INTRODUCTION

THE recent availability of large lithium-drifted germanium detectors has prompted intensive re-examination of neutron-capture γ -ray experiments. Resolution of the order of 6-10 keV is attainable for 6-MeV γ rays using commercially available detectors and electronics. This resolution is more than an order of magnitude better than that attainable with NaI(Tl), and is sufficient to fully resolve most transitions from a capturing state at 5-8 MeV to levels of low excitation in the final nucleus, even in the heavy elements. Therefore a great deal of valuable information can be obtained by utilizing these new detectors in studies of the high-energy γ rays which are emitted following neutron capture in individual resonances of medium- and heavy-mass target nuclei. It has been shown by Wasson *et al.* that Ge(Li) capture γ -ray spectra can be obtained with a thermalized flux

of neutrons from Pu-Be sources,¹ and in both the thermal and the resonance-energy region with neutrons produced by a linear accelerator.² These same kinds of experiments should also be possible using a facility with low γ -ray and low fast-neutron backgrounds, incorporating the "through" hole in the Materials Testing Reactor. The present studies were done in part to verify that the neutron flux from this facility is sufficient to investigate resonance neutron-capture γ -ray spectra with a germanium detector. The target for these initial studies was chosen with the idea of thoroughly testing the capabilities of the apparatus. A natural-tungsten target seemed to meet this requirement. Naturally occurring tungsten consists of several isotopes with roughly equal abundances. Three of these isotopes have at least one low-lying

¹ O. A. Wasson, K. J. Wetzel, and C. K. Bockelman, *Phys. Rev.* **136**, B1640 (1964).

² K. J. Wetzel, O. A. Wasson, and C. K. Bockelman, *Bull. Am. Phys. Soc.* **10**, 13 (1965).

* Work performed under the auspices of the U. S. Atomic Energy Commission.

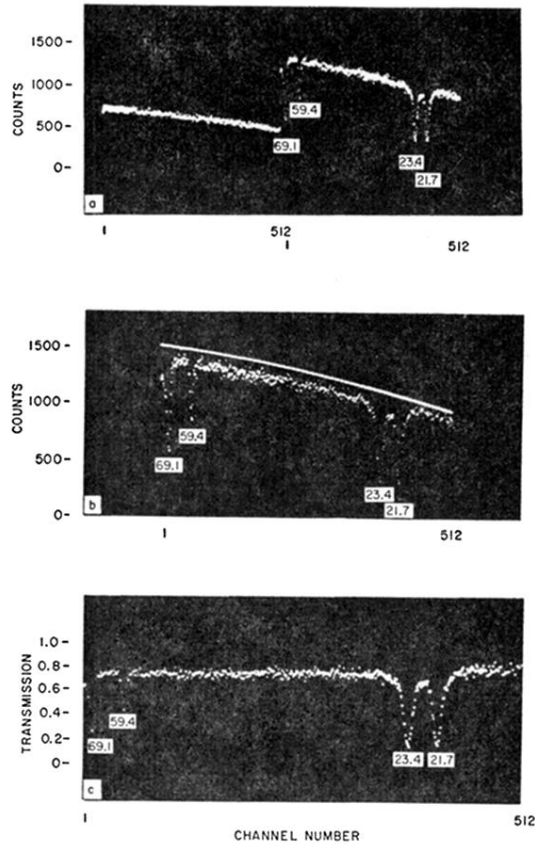


FIG. 2(a). The sample-out and sample-in time-of-flight spectra for the $\frac{1}{8}$ -in.-thick thorium sample. The open spectrum run time was approximately half of the sample run time. Each spectrum contains 512 0.5- μ sec channels, and the resonance energies are shown in eV. (b) The sample-out and sample-in spectra are shown after fitting a second degree polynomial to the open spectrum and normalizing to the equivalent running time of the sample spectrum. The spectra are shown superposed. (c) The computed transmission obtained from spectra of Fig. 2(b). The energy range shown is from about 75 to 20 eV.

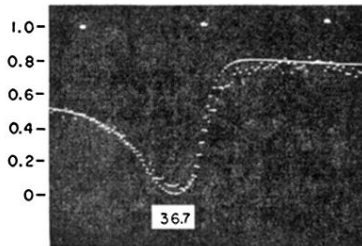
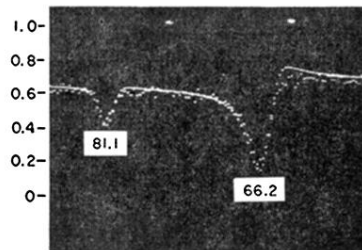
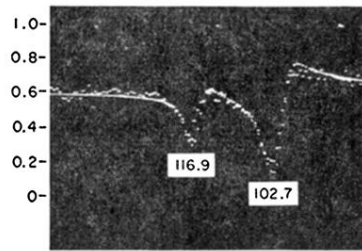


FIG. 3. Time-of-flight spectra for five resonances in ^{238}U at $E_0 = 117, 103, 81, 66,$ and 37 eV. The fitted curves show clearly discrepancies between measured and calculated transmissions, particularly at or near the maximum and minimum transmission regions.

FIG. 4. Spectra similar to those of Fig. 3, except for the use of a non-Gaussian resolution function, which clearly improves the fit.

